

# Rediscovery of the Effectiveness of Standard Convolution for Lightweight Face Detection

Joonhyun Jeong

Beomyoung Kim

Joonsang Yu

Youngjoon Yoo

NAVER CLOVA

{joonhyun.jeong, beomyoung.kim, joonsang.yu, youngjoon.yoo}@navercorp.com

## Abstract

This paper analyses the design choices of face detection architecture that improve efficiency between computation cost and accuracy. Specifically, we re-examine the effectiveness of the standard convolutional block as a lightweight backbone architecture on face detection. Unlike the current tendency of lightweight architecture design, which heavily utilizes depthwise separable convolution layers, we show that heavily channel-pruned standard convolution layer can achieve better accuracy and inference speed when using a similar parameter size. This observation is supported by the analyses concerning the characteristics of the target data domain, face. Based on our observation, we propose to employ ResNet with a highly reduced channel, which surprisingly allows high efficiency compared to other mobile-friendly networks (e.g., MobileNet-V1, -V2, -V3). From the extensive experiments, we show that the proposed backbone can replace that of the state-of-the-art face detector with a faster inference speed. Also, we further propose a new feature aggregation method maximizing the detection performance. Our proposed detector EResFD obtained 80.4% mAP on WIDER FACE Hard subset which only takes 37.7 ms for VGA image inference in on CPU. Code will be available at <https://github.com/clovaai/EResFD>.

## 1. Introduction

Face detection research experienced significant performance improvement after advent of recent deep neural network based general object detection approaches such as one-stage detector (e.g., SSD [1], YOLO [2], RetinaNet [3], EfficientDet [4]) and two-stage detector (e.g., Faster R-CNN [5], FPN [6], Mask R-CNN [7], Cascade R-CNN [8]). For applicable in a real-world scenario, real-time face detection has attracted more attention, and recent face detectors commonly adopt the one-stage approach that is more simple and efficient than the two-stage approach.

Recent studies for real-time face detection methods fre-

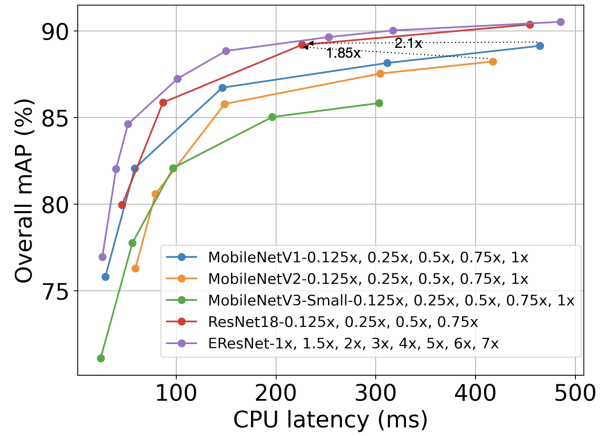


Figure 1. Latency-Accuracy pareto curve. We investigate the latency trend of various backbones including MobileNets family and ResNet according to adjusting width multiplier on RetinaFace [9] framework. ResNet shows much lower latency compared with MobileNet family even though its mAP is higher than others. One step forward to the observation, we propose a modified ResNet backbone for face detection task, abbreviated as EResNet, which reports superior face detection performance among other backbones.

quently use the lightweight model consisting of depth-wise separable convolution, which is used in MobileNet [10] and ShuffleNet [11]. Specifically, a line of recent lightweight face detectors including RetinaFace [9], SCRFD [12], CR-Face [13]) employ the MobileNet-V1 architecture [14] as the backbone network and reduce the number of channels in depthwise separable convolution layers by adjusting the width mutliplier. Following the paradigm of residual block [15], BlazeFace [16] proposes BlazeBlock that consists of depthwise separable convolution layers with skip connection, achieving a stronger performance. In practice, adopting the depthwise separable convolution is a reasonable choice to save the number of floating point operations (FLOPs), which is one of the important measurement for the real-time application. Summing up the following common practice, most real-time face detectors utilize the depthwise

separable convolution layers in their model by default.

In this paper, we rethink the common belief for the depthwise separable convolution layer and found out that the standard convolution with reducing the number of channels can achieve a better trade-off between latency and detection performance than depthwise separable convolution. Here, we use ResNet18 [15] as our baseline backbone network for the standard convolution and compare with the depthwise separable convolution based backbone networks (MobileNetV1 [10], MobileNetV2 [17], and MobileNetV3 [18]). Figure 1 shows the latency and average of mean average precision (mAP) scores on WIDER FACE [19] Easy, Medium, and Hard subsets. ResNet18 demands much higher latency than MobileNet when width multiplier is not applied. However, ResNet18 becomes much faster than MobileNet with higher mAP when reducing the number of channels using the width multiplier. Note that ResNet18-0.5x denotes that width multiplier 0.5 is applied, and it is 2.1 times faster than MobileNetV1-1.0x and 1.85 times faster than MobileNetV2-1.0x even though its mAP is higher than others.

Based on the observation, we propose EResFD, which is ResNet based real-time face detector. We firstly propose a slimmed version of ResNet architecture, namely EResNet, by redesigning the new stem layer, and changing the block configuration. Those methods can effectively reduce the inference latency and achieve higher detection accuracy compared with ResNet18. Secondly, we also propose the new feature map enhancement modules; Separated Feature Pyramid Network (SepFPN) and Cascade Context Prediction Module (CCPM). SepFPN aggregates information from high level and low level feature maps separately, and CCPM further effectively captures diverse receptive fields by employing a cascade design. Equipped with these architectural designs, our EResFD achieved 3.1% higher mAP on WiderFace Hard subset compared to the state-of-the-arts lightweight face detectors such as FaceBoxes [20].

We summarize the main contributions as follows:

- We propose a ResNet-based extremely lightweight backbone architecture, which is much faster than previous work on the CPU and mobile device achieving the state-of-the-art detection performance.
- We analyze the behavior of both standard convolution and depthwise separable convolution, and we found that the standard convolution is much faster than the depthwise separable convolution under extremely lightweight condition.
- We propose a channel dimension preserving strategy to reduce the latency, fitting the number of layer in each layer group to recover the performance degeneration.
- We propose a latency-aware enhance module, SepFPN

and CCPM. These enhance modules enable to improve the detection performance on all (large, medium, small) face scales, with much faster speed compared to previous feature enhance modules.

## 2. Related Works

**Face Detectors** Recent face detectors [9, 13, 16, 21–37] achieved impressive performance enhancement. These face detectors apply the architectural improvement of the general object detectors such as SSD [1] and RetinaNet [3] or two-stage detectors such as Faster R-CNN [5] and FPN [6]. The improvement of the face detection enabled to detect faces with various density and scales. To detect dense and small-scaled faces, current state-of-the-art group of detectors [9, 13, 23–25, 27, 33, 38] mostly employ large-scaled classification networks with custom-designed upsampling blocks. Besides the ResNet families [15], prototypical choice, various attempts including those from architecture search [36] has been applied. PyramidBox series [23, 27] and DSFD [38] suggested own upsampling blocks to improve the expressiveness of the features for dealing with finer faces. RetinaFace [9], currently dominant one, infers five-point keypoint landmarks of the faces: eyes, nose, mouth, in addition to the detection box, similar to MTCNN [39]. HAMBox [33] focuses on unmatched box which can be used for further performance improvement. The large memory size requirements of the face detectors critically hinder their applicability on edge-devices. Here, we target on reducing the weight parameters of the backbone network to increase the usability of the face detectors.

**Lightweight Face Detectors** To run the above mentioned face detectors on mobile or CPU devices, some of the detectors provide their lighter version, mostly substituting their backbones to lighter classification networks utilizing depthwise convolution [14]. After advent of the pioneering works from MobileNet-V1 [14] and V2 [17] utilizing depthwise separable convolution and inverted bottleneck block, more refinements [18, 40–43] on the architectures have brought the performance enhancements. These architectures show the competitive ImageNet [44] classification accuracy to larger classification models and also for the transferred tasks like object detection [1, 5] and segmentation [45]. Following the improvement of the lightweight backbone networks, RetinaFace [9] and SCRFD [13] use channel-width pruned version of MobileNet [14]. BlazeFace [16] and MCUNetV2 [46] proposed new variants of MobileNet targeting on mobile GPU and CPU environment, and EXTD [32] recursively uses the inverted bottleneck block of the MobileNet for further slimming the network size. Besides the overall tendency of using depthwise separable convolution based backbones, KPNet [37] proposes its own backbone network consisting of standard convolutional

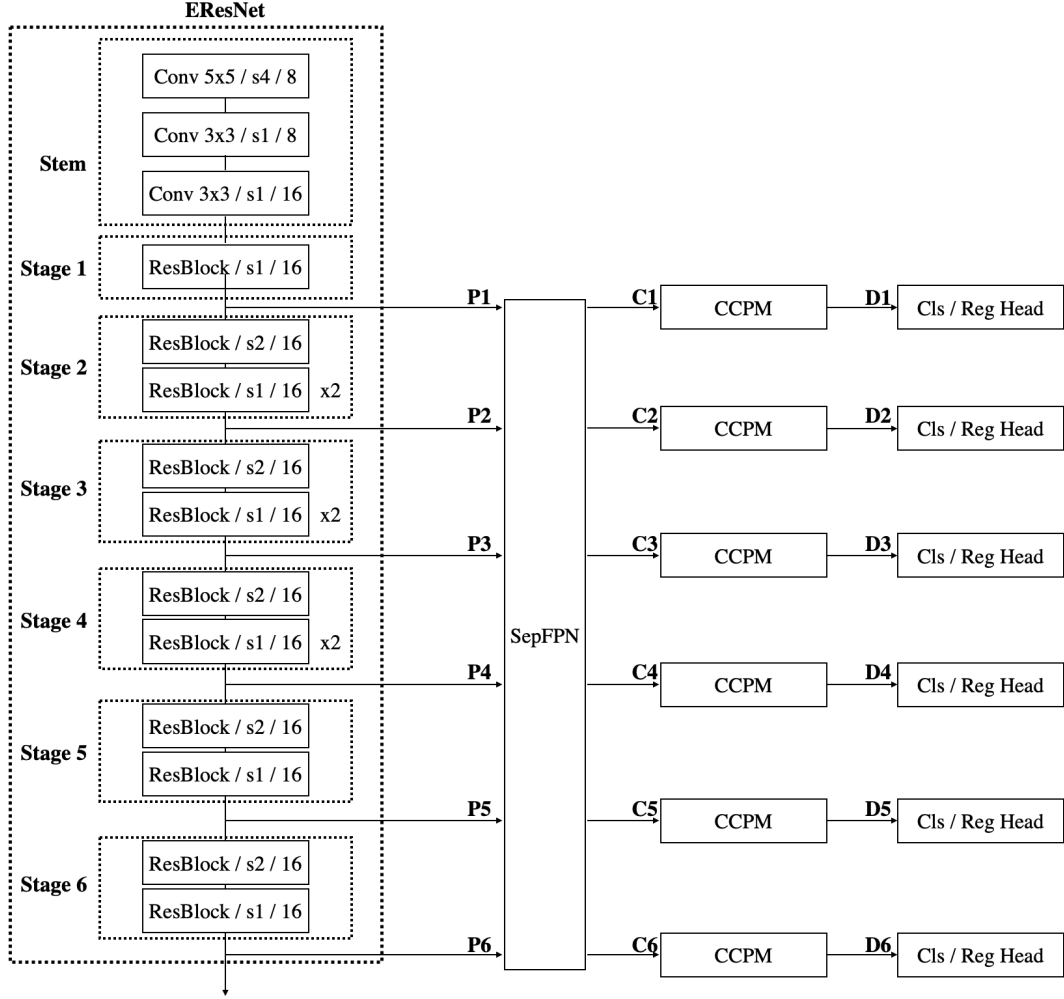


Figure 2. Entire architecture of EResFD. The proposed architecture consists of EResNet with 31 weighted layers, and SepFPN and Cascade Context Prediction Module (CCPM) are also introduced. ResBlock denotes basic residual block, which proposed in [15]. The first ResBlock of each stage has stride of 2, and every ResBlock has the same number of output channels as 16 in case of EResFD-1x. For the classification and regression head, single 1x1 convolution layer is used.

network, but its size is still large for edge devices, about 1 million parameters, and focuses on sparse and large scaled faces. In this paper, we rediscover the efficiency of standard convolution layers, which can cover faces with various scale and density, under extremely lightweight model size and minimal inference time.

### 3. EResFD

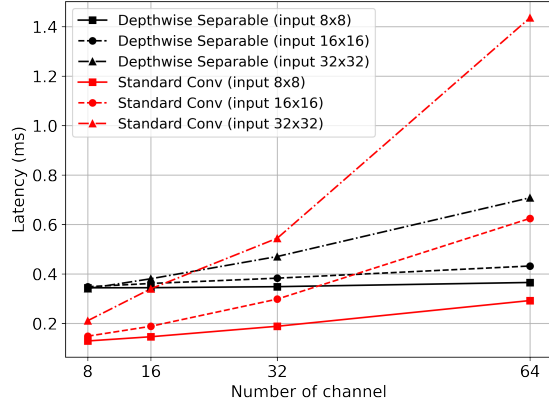
As we mentioned in Section 1, ResNet achieves both the faster inference time and higher detection performance. From this observation, we revisit the ResNet architecture. Figure 2 illustrates the proposed face detection architecture, named as efficient-ResNet (EResNet) based Face Detector, EResFD. It consists of two main parts; modified ResNet backbone architecture and newly proposed feature

enhancement modules. We modify several parts of ResNet to reduce the latency while preserving the detection performance based on empirical analysis on the network, and we also propose both the new feature pyramid module and context prediction module, which are called Separated Feature Pyramid Network (SepFPN) and Cascade Context Prediction Module (CCPM), respectively. Both modules improve the detection performance, and also show comparable or even faster latency compared with previous state-of-the-arts CPU detectors [47, 48].

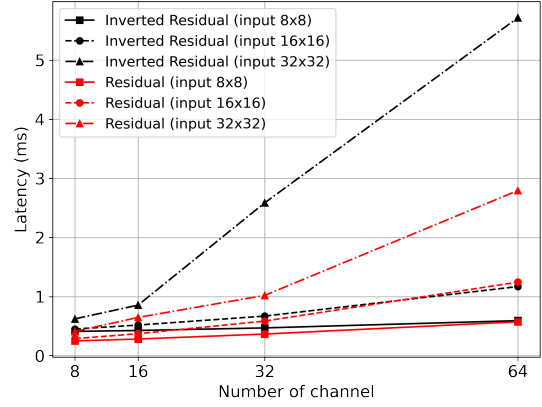
#### 3.1. Rethinking ResNet Architecture

##### 3.1.1 Convolutional Layer Analysis

Depthwise separable convolution is introduced to reduce the multiplication and accumulation cost of the convolu-



(a) standard convolution vs depthwise separable convolution



(b) residual block (ResNet) vs inverted bottleneck block (MobileNet-V2)

Figure 3. Illustration of latency comparison with varying channel size: (a) standard and depthwise separable convolution, (b) residual block (ResNet) and inverted bottleneck block (MobileNet-V2).

Table 1. Comparison of computational cost between standard and depthwise separable convolution. We calculate the FLOPs count for three kinds of setting, and each value indicates the multiply-add count for single layer.

Type	Standard	Depthwise Separable	
Operation	3x3 Conv	Depthwise Conv	Pointwise Conv
FLOPs (H,W=16, C=16)	1.18M	0.07M	0.13M
FLOPs (H,W=16, C=32)	4.71M	0.15M	0.52M
FLOPs (H,W=16, C=64)	18.87M	0.29M	2.10M

tion, which occupy most of computation time during the inference. Table 1 shows the comparison of computational cost between the standard and depthwise separable convolution for each stage. Depthwise separable convolution has much smaller FLOPs, and hence it can significantly reduce the computational cost. However, previous work [49] claims that FLOPs is not always matched with actual latency. Latency can be bounded by memory access and hardware accelerator, *i.e.*, CPU or GPU, so the target hardware characteristic should be considered for the architecture design.

To check the relationship between FLOPs and latency, we investigate the behavior of both standard convolution and depthwise separable convolution on CPU. We measured the latency of both convolutional layers on CPU, and Figure 3a shows the comparison result. Considering faster inference with small-sized input image (*e.g.*, less than 320x), we tested with input sizes 8x8, 16x16, and 32x32. As input size increases, the latency of standard convolution is steeply increasing, but depthwise separable convolution shows the small amount of latency growth. However, stan-

dard convolution achieves smaller latency than depthwise separable convolution on the extremely light weight condition. For all the input sizes, standard convolution is faster than depthwise separable convolution when its channel dimension is equal to or smaller than 16 as shown in Figure 3a. Since ResNet and MobileNetV1 each consists of standard convolution and depthwise separable convolution, we can safely conclude that ResNet has a chance to become faster than MobileNetV1 when we extremely reduce the channel size.

Furthermore, we also analyze the block level behavior of each convolutional layer. We use residual block and inverted residual block, which consist of standard and depthwise separable convolution, respectively. The residual block consists of two standard 3x3 convolution. MobileNet-V2 has inverted residual block, which includes one depthwise convolution and two pointwise convolution. Inverted residual block commonly expand the number of channels for the depthwise convolution, which is called expansion ratio. In MobileNet-V2, expansion ratio is set to 6 for most inverted residual blocks [17], which is reported to preserve the classification ability of the block compared to standard convolution counterpart [50]. Here, we use the equivalent expansion ratio for the latency comparison. Figure 3b shows the block level latency, and we found that residual block is much faster than inverted residual block in most cases. Residual block has 9.43M FLOPs and inverted residual block has 7.18M FLOPs when input size is 16x16 and the number of channels is 32. Even though residual block has more multiply-add operations, its latency is faster than inverted residual block.

The latency trend of each layer and block shows that standard convolution has a chance to surpass the depthwise separable convolution according to the latency. This trend is

Table 2. Latency breakdown of ResNet18-0.25x model. Stem denotes 7x7 convolution layer followed by maxpool layer, which reduces spatial size by 4 times. For Stage 1 ~ 4, strides of output feature map are set to 4 ~ 32.

Component	Latency (ms)	Ratio (%)
Stem	24.1	44
Stage 1	10.5	19
Stage 2	7.5	13
Stage 3	6.6	12
Stage 4	6.5	12
Total	55.2	100

Table 3. Latency of stem layers on ResNet18-0.25x model. Ratio denotes the portion of stem latency compared to the overall network latency.

Stem	ResNet	EResNet
Stem FLOPs	180.6 M	11.5 M
Stem Latency (Ratio)	24.1ms (44%)	4.5ms (13%)

also the same on network level analysis as we mentioned in Section 1. Therefore, we propose efficient backbone originated from the ResNet.

### 3.1.2 Stem Layer Modification

We analyze the ResNet architecture, and we observed that stem layer occupies large amount of entire latency. Table 2 shows the latency breakdown of ResNet-18 with width multiplier 0.25, and it shows that almost half of total latency is originated from stem layers. The backbone network is highly lightened by applying the small width multiplier, so proportion of stem layer becomes larger. Moreover, ResNet stem layer consists of 7x7 convolution with stride of 2, so it requires large amount of computation compared than others. The number of computation (FLOPs) is proportional to square of kernel size ( $K^2$ ) and reciprocal-square of stride ( $1/S^2$ ). If kernel size is reduced to 5, its FLOPs becomes about 50% of 7x7 convolution, and FLOPs further decrease to about 13% when its stride of 4 is applied simultaneously.

To reduce latency of stem layers, we first change stride to 4 for the convolutional layer, which is already adopted in the previous work [47]. We also reduce the kernel size from 7 to 5, but it can hurt the detection performance because it is directly related to receptive field. To alleviate this problem, we introduce two additional convolutional layers right after 5x5 convolution. Thanks to those convolutional layers, receptive field size becomes larger than original stem layer, but its computation complexity is still much lower than original. Table 3 shows comparison results on the stem layer. By adopting smaller kernel size and bigger stride, EResNet stem layer has much smaller FLOPs, and also achieves

Table 4. Latency breakdown of ResNet18 models where channels are doubled or preserved for stage 2,3,4. Width multiplier is set to be 0.25 for ResNet-preserved model to keep number of output channels as 16 for all the stages.

Model	ResNet	ResNet-Preserved
Stage 2	Latency (ms)	7.5
	FLOPs (M)	157.3
Stage 3	Latency (ms)	6.6
	FLOPs (M)	157.3
Stage 4	Latency (ms)	6.5
	FLOPs (M)	157.3

much shorter latency compared with ResNet stem layer.

### 3.1.3 Architecture Re-Configuration for Face

In modern backbone architecture, The number of channels is continuously increasing from bottom to top layer [15, 42, 51]. In ResNet, for example, channel dimension is doubled when its spatial dimension is decreased (stride of 2). This designing trend is based on that high-level features are highly related to the specific classes [52]. When the number of object classes increases, high-level feature dimension has to be enlarged. However, there is only one object class in the face detection task, so we suppose that the channel dimension may be reduced compared with object detection task.

To accelerate face detection speed, EResNet backbone is designed by reducing the number of channels. From the assumption, we propose the channel dimension preserving strategy, which means that we do not double the channel dimension for every stage. Table 4 shows the number of FLOPs and latency when our channel preserving strategy is applied, and it shows that our method significantly reduced the latency and FLOPs of each stage. We note that the number of FLOPs is also proportional to input and output channel dimension, and hence the amount of the reduction is huge. Latency reduction amount is not as large as FLOPs reduction, but it is still remarkable. As already shown in Figure 2, we set the channel dimension of our EResNet architecture to 16.

The network capacity also decreases due to the channel dimension reduction, so we adjust stage configuration to compensate the performance degeneration. Figure 2 shows the detailed stage configurations. We insert one more blocks for the stage 2~4 to improve small face detection performance, and add two extra stages (stage 5 and 6) for the large face. The number of residual block increases from 8 to 14, so additional residual block can increase the inference time. However, the channel preserving strategy significantly reduce FLOPs, and the computational cost of each block is

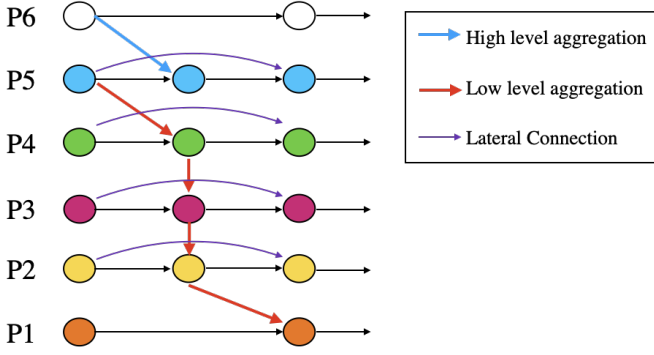


Figure 4. Architecture of SepFPN. High level features and low level features are aggregated separately, based on fast-normalized fusion [54]. Also, final output node is fused with original input node (*i.e.*, lateral connection), following [54].

also much smaller than original residual block. For this reason, EResNet architecture is still much faster than baseline ResNet architecture as shown in Figure 1.

### 3.2. Feature Enhance Modules

#### 3.2.1 SepFPN

To improve the detection performance for small objects, feature pyramid network (FPN) [6] is widely used. FPN propagates context of high-level feature into low-level feature (top-down) to strengthen the feature information for the small object. However, previous work claimed that aggregating high-level feature onto low-level feature can hurt detection performance for small face because receptive field of high-level feature is too large for the small face [23]. Also, the state-of-the-art object detectors use not only top-down but also bottom-up path [53, 54], which can induce large latency overhead on FPN module.

To resolve the problems, we propose the a FPN module, separated feature pyramid network (SepFPN). As illustrated in Figure 4, we remove the bottom-up path to reduce the latency overhead from the BiFPN [54], and preserve the lateral connection for the feature aggregation. Features are aggregated with a simple element-wise weighted summation [54], so its latency overhead is negligible. Also, we change the top-bottom aggregation method. From the previous observation [23], we assume that large difference of receptive field among each aggregation group causes performance degeneration for the feature aggregation. Based on this intuition, we adopt the two separated top-bottom path to let each aggregation group have similar receptive field. While low-level feature aggregation has been demonstrated to noticeably improve detection performance for the small face detection [23], we claim that high-level feature aggregation also makes a improvement of large face detection.

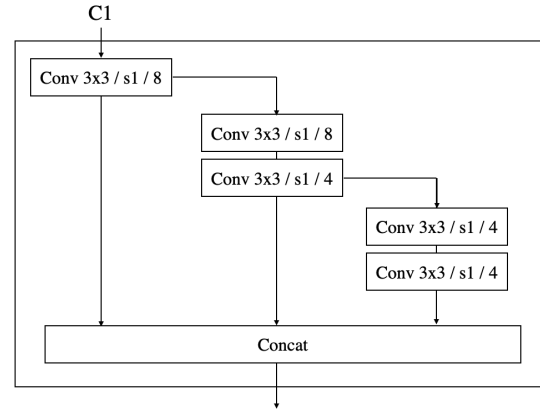


Figure 5. Architecture of CCPM in case of EResFD-1x. We only visualize CCPM for feature map C1 in Figure 2 for simplicity.

#### 3.2.2 CCPM

To supplement the feature information, we also provide cascade context prediction module (CCPM), a latency-aware context module design. The context prediction module is proposed to expand the receptive field [22], and we also design CCPM to achieve the equivalent purpose. Figure 5 shows our CCPM architecture. The cascade structure can enrich larger size of receptive field than previous work [22], while ensuring faster speed than the previous heavy-weight enhance modules using densely connected convolution layers [27] and convolution layers with large asymmetric kernel [55]. Thanks to this advantages, CCPM achieves lower latency with comparable detection performance.

## 4. Experiment

In this section, we evaluate our proposed EResFD by analyzing effectiveness of each component of EResFD and by comparing with the state-of-the-art (SOTA) face detectors. For quantitatively measuring accuracy of detection, we used WIDER FACE [19] dataset. For training on WIDER FACE, color distortion, zoom-in and out augmentation, max-out background label, multi-task loss are used, following S3FD [21]<sup>1</sup>. For evaluation, we employed flip and multi-scale testing [21], where all these predictions are merged by Box voting [56] with intersection-over-union (IoU) threshold at 0.3. In case of using RetinaFace framework [9]<sup>2</sup>, we used single-scale testing where original image size is maintained. For measuring latency, we used Intel Xeon CPU (E5-2660v3@2.60 GHz) with VGA input resolution (480×640).

<sup>1</sup>We obtained source code from <https://github.com/yxlijun/S3FD.pytorch>

<sup>2</sup>We obtained source code from [https://github.com/biubug6/Pytorch\\_Retinaface](https://github.com/biubug6/Pytorch_Retinaface)

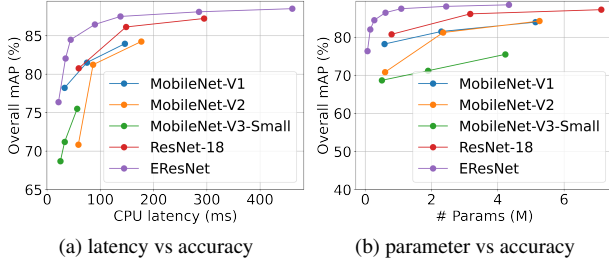


Figure 6. Performance comparison of various backbone networks in terms of CPU latency and number of parameters. We applied width multipliers 1x, 1.5x, 2x, 3x, 4x, 6x, 8x for EResNet. For the other backbones, we applied width multiplier 0.25x, 0.5x, 0.75x.

Table 5. Performance comparison of various FPN modules on WIDER FACE.

Model	Latency (ms)	mAP (%)			
		Easy	Medium	Hard	Overall
EResNet	20.9	85.09	82.78	61.20	76.36
+ FPN [6]	24.0	85.30	84.25	75.45	81.67
+ LFPN [23]	23.8	85.24	84.21	76.58	82.01
+ PANet [53]	35.5	87.96	86.82	77.95	84.24
+ BiFPN [54]	35.6	87.16	85.95	77.56	83.56
+ SepFPN (Ours)	27.0	87.68	86.30	77.68	83.89

#### 4.1. Component Study

**Backbone Network.** Figure 6 shows the comparison result for widely used light-weight backbone; ResNet-18, MobileNet V1, V2, and V3. The experimental results show that EResNet achieved superior inference latency given the same mAP condition and also has higher mAP given the same latency condition, as shown in Figure 6a. Our proposed stem layer and channel dimension preserving strategy are shown to be very helpful for the latency reduction, while maintaining the powerful face detection performance. In addition, EResNet also outperformed other comparison methods in terms of the number of parameters. In Figure 6b, EResNet shows the highest mAP with much smaller number of parameters. To further prove general effectiveness of EResNet backbone, we additionally compared with various backbone architectures on RetinaFace framework in Figure 1. For all the backbones, we only employed 3 detection heads from P2 ~ P4 in Figure 2, following [9]. The results further corroborate that our EResNet architecture has the best latency-accuracy trade-off among the various backbones. From those experiments, we found that the proposed methods effectively reduce both latency and parameters without causing mAP degeneration.

**SepFPN.** We measure the detection performance and latency of several FPN modules on the EResNet backbone, and Table 5 shows the comparison result. Thanks to the

Table 6. Ablation study of SepFPN with various separation position. In case of separation position is 5 (Figure 4), high level features are only aggregated from P6 to P5 and the rest low-level features are aggregated from P5 to P1.

Separation Position	Latency (ms)	mAP (%)			
		Easy	Medium	Hard	Overall
P3	26.9	85.95	84.39	75.31	81.88
P4	26.7	87.16	85.70	77.12	83.33
P5	27.0	87.68	86.30	77.68	83.89

Table 7. Performance comparison of various Feature Enhance Modules before detection head on WIDER FACE. For fair comparisons, we fix baseline backbone network as EResNet-1x equipped with LFPN [23].

Model	Latency (ms)	mAP (%)			
		Easy	Medium	Hard	Overall
Baseline	23.8	85.24	84.21	76.58	82.01
+ SSH [22]	35.5	87.49	86.34	79.28	84.37
+ CPM [23]	42.4	87.47	86.74	80.00	84.74
+ FEM [24]	41.5	86.90	86.15	79.22	84.09
+ DCM [27]	48.1	87.48	86.51	79.85	84.61
+ CCPM (ours)	<b>33.8</b>	87.25	86.38	79.90	84.51

bottom-up aggregation path, PANet [53] and BiFPN [54] have much higher mAP than others. However, SepFPN achieves comparable or higher detection performance than both PANet and BiFPN although SepFPN does not have any bottom-up path. This experiment shows that bottom-up path would not be an essential block for the face detection performance, and about 42% of the FPN latency can be reduced by removing the bottom-up path. We further empirically studied on the separation position of SepFPN, and Table 6 shows the result. The latency is not significantly affected from separation position, but the accuracy is very sensitive according to the separation position. We observed that P5 achieves best mAP for all different kinds of face size, and hence we applied P5 for all other experiments.

**CCPM.** Table 7 shows comparison result of the effect of various feature enhance modules. The feature enhance module makes large performance gain, but several previous works [23, 24, 27] show similar detection performance. Our CCPM module mainly focuses on latency reduction, and experimental result shows that CCPM achieves the smallest latency, satisfying the purpose. In addition, CCPM also achieves higher overall mAP than SSH, which is the fastest among all the previous methods mentioned in the Table.

#### 4.2. Comparison with SOTA Detectors

We compare our proposed method with the SOTA real-time CPU detectors on WIDER FACE validation dataset. Table 8 shows the comparison result. **EResNet-1x** indi-

Table 8. Comparison with previous works on WIDER FACE validation set. All models are evaluated with multi-scale testing, following [9, 21]. For measuring FLOPs and Latency, VGA resolution (480×640) is used. For MTCNN, we used input sizes designated by [57].

Method	Backbone	Feature Enhance Module	# Params	# FLOPs	Latency	mAP (%)			
						Easy	Medium	Hard	Overall
MTCNN [57]	P-,R-,O-Net [57]	-	0.12M	14M	4.0ms	85.10	82.00	60.70	75.93
FaceBoxes [47]	FaceBoxes [47]	FPN + DCH	0.66M	156M	35.7ms	88.50	86.20	77.30	84.00
RetinaFace [9]	MobileNetV1-0.25x [14]	FPN + SSH	0.42M	754M	58.5ms	88.67	87.09	<b>80.99</b>	85.58
EResFD	<b>EResNet-1x</b>	-	0.07M	228M	20.9ms	85.09	82.78	61.20	76.36
EResFD	<b>EResNet-1x</b>	<b>SepFPN</b>	0.08M	250M	27.0ms	87.68	86.30	77.68	83.89
EResFD	<b>EResNet-1x</b>	<b>SepFPN + CCPM</b>	0.09M	298M	37.7ms	<b>89.02</b>	<b>87.96</b>	80.41	<b>85.80</b>

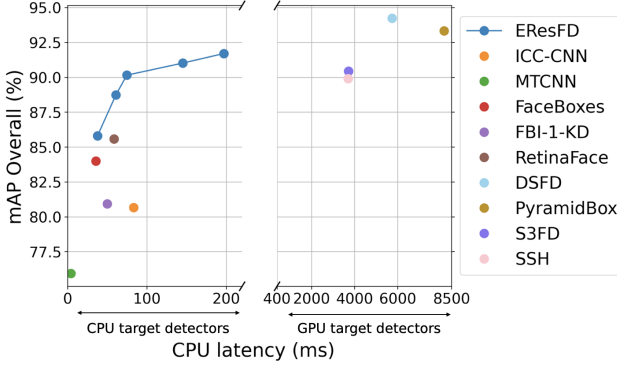


Figure 7. Performance comparison of EResFD with other SOTA CPU target detectors [9, 47, 48, 57, 58] and GPU target detectors [21–24, 59]. For RetinaFace [9], MobileNetV1-0.25x backbone was used.

cates EResNet backbone architecture shown in Figure 2, with width multiplier 1. In case of RetinaFace [9] backbone, width multiplier 0.25 is applied. MTCNN shows the smallest FLOPs and Latency, but it has large mAP degradation for medium and hard case. EResFD has the smallest number of parameters, and also achieves the highest overall mAP. The latency of EResFD is similar to that of FaceBoxes [20], but its detection performance is much higher. Moreover, proposed method achieves similar or slightly higher mAP compared with RetinaFace [9], but its latency is about 64% of RetinaFace.

Table 8 (bottom part) also shows the ablation study for the proposed modules; SepFPN and CCPM. SepFPN improves the overall mAP about 7.5%, but its latency only increases by 6ms. Moreover, we also achieve 1.9% overall mAP improvement when CCPM is further applied. We observed that proposed modules can make a large performance improvement even when jointly applied.

In addition, we also compare the latency and detection performance with other CPU and GPU target face detectors in Figure 7. As we already mentioned above, our method achieves the highest mAP among all the CPU target face detectors. In addition, we found that it also shows comparable detection performance compared with GPU target detectors. EResFD shows the similar detection accuracy with S3FD and SSH, but it is about 19x faster.

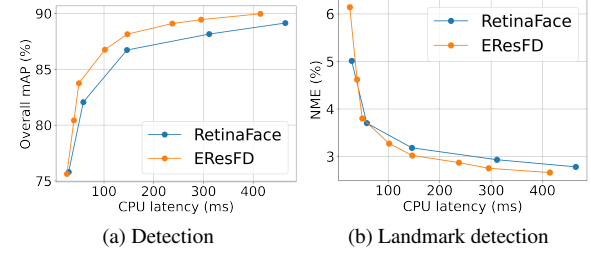


Figure 8. Performance of face detection on WIDER FACE and landmark detection on AFLW [60] dataset. Based on RetinaFace framework where face bounding boxes with facial landmarks can be jointly detected, we only replaced backbone network from MobileNet-V1 to EResNet, while FPN and SSH are replaced by our proposed SepFPN and CCPM, respectively for EResFD.

Furthermore, we compare the proposed method with RetinaFace, one standard lightweight face detector in this field. Since RetinaFace detects face and facial landmarks at the same time, we covered the landmark detection as well. We measure the face detection performance on WIDER FACE and landmark detection performance on AFLW. Figure 8 shows comparison on the face and landmark detection. The results show that our EResFD achieves higher mAP for face detection task and lower NME for the landmark detection task.

## 5. Conclusion

This paper re-highlights the efficiency of standard convolution-based architecture for the lightweight face detection. The extensive experimental results showed that the standard convolutional block achieved superior performance compared to depthwise separable convolution, contrary to the common trend in this field. Based on the observation, we propose an efficient architecture EResNet, which includes modified stem layer and channel dimension preserving strategy. Also, we propose SepFPN and CCPM for the feature enhancement, which boosts the detection performance without sacrificing latency and parameter size. Finally, summing up the observations and architecture suggestions for face detection, we establish a new state-of-the-art real-time CPU face detector, EResFD, achieving the SOTA face detection performance among the lightweight detectors.

## References

- [1] W. Liu, D. Anguelov, D. Erhan, C. Szegedy, S. Reed, C.-Y. Fu, and A. C. Berg, “Ssd: Single shot multibox detector,” in *European conference on computer vision*, pp. 21–37, Springer, 2016. [1](#), [2](#)
- [2] J. Redmon, S. Divvala, R. Girshick, and A. Farhadi, “You only look once: Unified, real-time object detection,” in *Proceedings of the IEEE conference on computer vision and pattern recognition*, pp. 779–788, 2016. [1](#)
- [3] T.-Y. Lin, P. Goyal, R. Girshick, K. He, and P. Dollár, “Focal loss for dense object detection,” in *Proceedings of the IEEE international conference on computer vision*, pp. 2980–2988, 2017. [1](#), [2](#)
- [4] M. Tan, R. Pang, and Q. V. Le, “Efficientdet: Scalable and efficient object detection,” in *Proceedings of the IEEE/CVF conference on computer vision and pattern recognition*, pp. 10781–10790, 2020. [1](#)
- [5] S. Ren, K. He, R. Girshick, and J. Sun, “Faster r-cnn: Towards real-time object detection with region proposal networks,” *Advances in neural information processing systems*, vol. 28, pp. 91–99, 2015. [1](#), [2](#)
- [6] T.-Y. Lin, P. Dollár, R. Girshick, K. He, B. Hariharan, and S. Belongie, “Feature pyramid networks for object detection,” in *Proceedings of the IEEE conference on computer vision and pattern recognition*, pp. 2117–2125, 2017. [1](#), [2](#), [6](#), [7](#)
- [7] K. He, G. Gkioxari, P. Dollár, and R. Girshick, “Mask r-cnn,” in *Proceedings of the IEEE international conference on computer vision*, pp. 2961–2969, 2017. [1](#)
- [8] Z. Cai and N. Vasconcelos, “Cascade r-cnn: Delving into high quality object detection,” in *Proceedings of the IEEE conference on computer vision and pattern recognition*, pp. 6154–6162, 2018. [1](#)
- [9] J. Deng, J. Guo, Y. Zhou, J. Yu, I. Kotsia, and S. Zafeiriou, “Retinaface: Single-stage dense face localisation in the wild,” *arXiv preprint arXiv:1905.00641*, 2019. [1](#), [2](#), [6](#), [7](#), [8](#), [11](#)
- [10] A. G. Howard, M. Zhu, B. Chen, D. Kalenichenko, W. Wang, T. Weyand, M. Andreetto, and H. Adam, “Mobilenets: Efficient convolutional neural networks for mobile vision applications,” *arXiv preprint arXiv:1704.04861*, 2017. [1](#), [2](#)
- [11] X. Zhang, X. Zhou, M. Lin, and J. Sun, “Shufflenet: An extremely efficient convolutional neural network for mobile devices,” in *Proceedings of the IEEE conference on computer vision and pattern recognition*, pp. 6848–6856, 2018. [1](#)
- [12] N. Vesdapunt and B. Wang, “Crface: Confidence ranker for model-agnostic face detection refinement,” in *Proceedings of the IEEE/CVF Conference on Computer Vision and Pattern Recognition*, pp. 1674–1684, 2021. [1](#)
- [13] J. Guo, J. Deng, A. Lattas, and S. Zafeiriou, “Sample and computation redistribution for efficient face detection,” *arXiv preprint arXiv:2105.04714*, 2021. [1](#), [2](#)
- [14] A. G. Howard, M. Zhu, B. Chen, D. Kalenichenko, W. Wang, T. Weyand, M. Andreetto, and H. Adam, “Mobilenets: Efficient convolutional neural networks for mobile vision applications,” *arXiv preprint arXiv:1704.04861*, 2017. [1](#), [2](#), [8](#)
- [15] K. He, X. Zhang, S. Ren, and J. Sun, “Deep residual learning for image recognition,” in *Proceedings of the IEEE conference on computer vision and pattern recognition*, pp. 770–778, 2016. [1](#), [2](#), [3](#), [5](#)
- [16] V. Bazarevsky, Y. Kartynnik, A. Vakunov, K. Raveendran, and M. Grundmann, “Blazeface: Sub-millisecond neural face detection on mobile gpus,” *arXiv preprint arXiv:1907.05047*, 2019. [1](#), [2](#)
- [17] M. Sandler, A. Howard, M. Zhu, A. Zhmoginov, and L.-C. Chen, “Mobilenetv2: Inverted residuals and linear bottlenecks,” in *Proceedings of the IEEE conference on computer vision and pattern recognition*, pp. 4510–4520, 2018. [2](#), [4](#)
- [18] A. Howard, M. Sandler, G. Chu, L.-C. Chen, B. Chen, M. Tan, W. Wang, Y. Zhu, R. Pang, V. Vasudevan, et al., “Searching for mobilenetv3,” in *Proceedings of the IEEE/CVF International Conference on Computer Vision*, pp. 1314–1324, 2019. [2](#)
- [19] S. Yang, P. Luo, C.-C. Loy, and X. Tang, “Wider face: A face detection benchmark,” in *Proceedings of the IEEE conference on computer vision and pattern recognition*, pp. 5525–5533, 2016. [2](#), [6](#)
- [20] S. Zhang, X. Wang, Z. Lei, and S. Z. Li, “Faceboxes: A cpu real-time and accurate unconstrained face detector,” *Neurocomputing*, vol. 364, pp. 297–309, 2019. [2](#), [8](#)
- [21] S. Zhang, X. Zhu, Z. Lei, H. Shi, X. Wang, and S. Z. Li, “S3fd: Single shot scale-invariant face detector,” in *Proceedings of the IEEE International Conference on Computer Vision*, pp. 192–201, 2017. [2](#), [6](#), [8](#), [11](#)
- [22] M. Najibi, P. Samangouei, R. Chellappa, and L. S. Davis, “Ssh: Single stage headless face detector,” in *Proceedings of the IEEE International Conference on Computer Vision*, pp. 4875–4884, 2017. [2](#), [6](#), [7](#), [8](#)
- [23] X. Tang, D. K. Du, Z. He, and J. Liu, “Pyramidbox: A context-assisted single shot face detector,” in *Proceedings of the European Conference on Computer Vision (ECCV)*, pp. 797–813, 2018. [2](#), [6](#), [7](#), [8](#)
- [24] J. Li, Y. Wang, C. Wang, Y. Tai, J. Qian, J. Yang, C. Wang, J. Li, and F. Huang, “Dsfd: dual shot face detector,” in *Proceedings of the IEEE Conference on Computer Vision and Pattern Recognition*, pp. 5060–5069, 2019. [2](#), [7](#), [8](#)
- [25] Y. Zhu, H. Cai, S. Zhang, C. Wang, and Y. Xiong, “Tinaface: Strong but simple baseline for face detection,” *arXiv preprint arXiv:2011.13183*, 2020. [2](#)
- [26] L. Cao, Y. Xiao, and L. Xu, “Emface: Detecting hard faces by exploring receptive field pyramids,” *arXiv preprint arXiv:2105.10104*, 2021. [1](#)
- [27] Z. Li, X. Tang, J. Han, J. Liu, and R. He, “Pyramidbox++: high performance detector for finding tiny face,” *arXiv preprint arXiv:1904.00386*, 2019. [2](#), [6](#), [7](#)

[28] F. Zhang, X. Fan, G. Ai, J. Song, Y. Qin, and J. Wu, “Accurate face detection for high performance,” *arXiv preprint arXiv:1905.01585*, 2019. [2](#)

[29] J. Zhu, D. Li, T. Han, L. Tian, and Y. Shan, “Progress-face: Scale-aware progressive learning for face detection,” in *European Conference on Computer Vision*, pp. 344–360, Springer, 2020. [2](#)

[30] M. Najibi, B. Singh, and L. S. Davis, “Fa-rpn: Floating region proposals for face detection,” in *Proceedings of the IEEE/CVF Conference on Computer Vision and Pattern Recognition*, pp. 7723–7732, 2019. [2](#)

[31] Y. Liu and X. Tang, “Bbbox: Searching face-appropriate backbone and feature pyramid network for face detector,” in *Proceedings of the IEEE/CVF Conference on Computer Vision and Pattern Recognition*, pp. 13568–13577, 2020. [2](#)

[32] Y. Yoo, D. Han, and S. Yun, “Extd: Extremely tiny face detector via iterative filter reuse,” *arXiv preprint arXiv:1906.06579*, 2019. [2](#)

[33] Y. Liu, X. Tang, J. Han, J. Liu, D. Rui, and X. Wu, “Hambox: Delving into mining high-quality anchors on face detection,” in *2020 IEEE/CVF Conference on Computer Vision and Pattern Recognition (CVPR)*, pp. 13043–13051, IEEE, 2020. [2](#)

[34] L. Ramos and B. Morales, “Swiftface: Real-time face detection,” *arXiv preprint arXiv:2009.13743*, 2020. [2](#)

[35] T. M. Hoang, G. P. Nam, J. Cho, and I.-J. Kim, “Deface: Deep efficient face network for small scale variations,” *IEEE Access*, vol. 8, pp. 142423–142433, 2020. [2](#)

[36] B. Zhang, J. Li, Y. Wang, Y. Tai, C. Wang, J. Li, F. Huang, Y. Xia, W. Pei, and R. Ji, “Asfd: Automatic and scalable face detector,” *arXiv preprint arXiv:2003.11228*, 2020. [2](#)

[37] G. Song, Y. Liu, Y. Zang, X. Wang, B. Leng, and Q. Yuan, “Kpnet: Towards minimal face detector,” in *Proceedings of the AAAI Conference on Artificial Intelligence*, vol. 34, pp. 12015–12022, 2020. [2](#)

[38] J. Li, Y. Wang, C. Wang, Y. Tai, J. Qian, J. Yang, C. Wang, J. Li, and F. Huang, “Dsfd: Dual shot face detector,” in *Proceedings of the IEEE Conference on Computer Vision and Pattern Recognition*, 2019. [2](#)

[39] K. Zhang, Z. Zhang, Z. Li, and Y. Qiao, “Joint face detection and alignment using multitask cascaded convolutional networks,” *IEEE Signal Processing Letters*, vol. 23, no. 10, pp. 1499–1503, 2016. [2](#)

[40] B. Wu, A. Wan, X. Yue, P. Jin, S. Zhao, N. Golmant, A. Gholaminejad, J. Gonzalez, and K. Keutzer, “Shift: A zero flop, zero parameter alternative to spatial convolutions,” in *Proceedings of the IEEE Conference on Computer Vision and Pattern Recognition*, pp. 9127–9135, 2018. [2](#)

[41] K. Han, Y. Wang, Q. Tian, J. Guo, C. Xu, and C. Xu, “Ghostnet: More features from cheap operations,” in *Proceedings of the IEEE/CVF Conference on Computer Vision and Pattern Recognition*, pp. 1580–1589, 2020. [2](#)

[42] M. Tan and Q. Le, “Efficientnet: Rethinking model scaling for convolutional neural networks,” in *International Conference on Machine Learning*, pp. 6105–6114, PMLR, 2019. [2](#)

[43] M. Tan and Q. V. Le, “Efficientnetv2: Smaller models and faster training,” *arXiv preprint arXiv:2104.00298*, 2021. [2](#)

[44] J. Deng, W. Dong, R. Socher, L.-J. Li, K. Li, and L. Fei-Fei, “Imagenet: A large-scale hierarchical image database,” in *2009 IEEE conference on computer vision and pattern recognition*, pp. 248–255, Ieee, 2009. [2](#)

[45] L.-C. Chen, Y. Zhu, G. Papandreou, F. Schroff, and H. Adam, “Encoder-decoder with atrous separable convolution for semantic image segmentation,” in *Proceedings of the European conference on computer vision (ECCV)*, pp. 801–818, 2018. [2](#)

[46] J. Lin, W.-M. Chen, H. Cai, C. Gan, and S. Han, “Mcunetv2: Memory-efficient patch-based inference for tiny deep learning,” *arXiv preprint arXiv:2110.15352*, 2021. [2](#)

[47] S. Zhang, X. Wang, Z. Lei, and S. Z. Li, “Faceboxes: A cpu real-time and accurate unconstrained face detector,” *Neurocomputing*, vol. 364, pp. 297–309, 2019. [3](#), [5](#), [8](#)

[48] H. Jin, S. Zhang, X. Zhu, Y. Tang, Z. Lei, and S. Z. Li, “Learning lightweight face detector with knowledge distillation,” in *2019 International Conference on Biometrics (ICB)*, pp. 1–7, IEEE, 2019. [3](#), [8](#)

[49] I. Bello, W. Fedus, X. Du, E. D. Cubuk, A. Srinivas, T.-Y. Lin, J. Shlens, and B. Zoph, “Revisiting resnets: Improved training and scaling strategies,” *Advances in Neural Information Processing Systems*, vol. 34, 2021. [4](#)

[50] D. Han, Y. Yoo, B. Kim, and B. Heo, “Learning features with parameter-free layers,” *arXiv preprint arXiv:2202.02777*, 2022. [4](#)

[51] C. Szegedy, S. Ioffe, V. Vanhoucke, and A. A. Alemi, “Inception-v4, inception-resnet and the impact of residual connections on learning,” in *Thirty-first AAAI conference on artificial intelligence*, 2017. [5](#)

[52] M. D. Zeiler and R. Fergus, “Visualizing and understanding convolutional networks,” in *European conference on computer vision*, pp. 818–833, Springer, 2014. [5](#)

[53] S. Liu, L. Qi, H. Qin, J. Shi, and J. Jia, “Path aggregation network for instance segmentation,” in *Proceedings of the IEEE conference on computer vision and pattern recognition*, pp. 8759–8768, 2018. [6](#), [7](#)

[54] M. Tan, R. Pang, and Q. V. Le, “Efficientdet: Scalable and efficient object detection,” in *Proceedings of the IEEE/CVF conference on computer vision and pattern recognition*, pp. 10781–10790, 2020. [6](#), [7](#)

[55] S. Zhang, C. Chi, Z. Lei, and S. Z. Li, “Refineface: Refinement neural network for high performance face detection,” *arXiv preprint arXiv:1909.04376*, 2019. [6](#)

[56] S. Gidaris and N. Komodakis, “Object detection via a multi-region and semantic segmentation-aware cnn model,” in *Proceedings of the IEEE international conference on computer vision*, pp. 1134–1142, 2015. [6](#), [11](#)

[57] K. Zhang, Z. Zhang, Z. Li, and Y. Qiao, “Joint face detection and alignment using multitask cascaded convolutional networks,” *IEEE Signal Processing Letters*, vol. 23, no. 10, pp. 1499–1503, 2016. [8](#)

- [58] K. Zhang, Z. Zhang, H. Wang, Z. Li, Y. Qiao, and W. Liu, “Detecting faces using inside cascaded contextual cnn,” in *Proceedings of the IEEE International Conference on Computer Vision*, pp. 3171–3179, 2017. [8](#)
- [59] Y. He, D. Xu, L. Wu, M. Jian, S. Xiang, and C. Pan, “Lffd: A light and fast face detector for edge devices,” *arXiv preprint arXiv:1904.10633*, 2019. [8](#)
- [60] M. Koestinger, P. Wohlhart, P. M. Roth, and H. Bischof, “Annotated facial landmarks in the wild: A large-scale, real-world database for facial landmark localization,” in *2011 IEEE international conference on computer vision workshops (ICCV workshops)*, pp. 2144–2151, IEEE, 2011. [8](#)
- [61] D. P. Kingma and J. Ba, “Adam: A method for stochastic optimization,” *arXiv preprint arXiv:1412.6980*, 2014. [11](#)

## A. Implementaion details

### A.1. Anchor Settings

As shown in Table 9, anchors whose sizes are ranged from 16 to 512 are assigned from detection layers from D1 to D6, following [21]. Anchor width ratio to the height is set to 1:1.25.

Table 9. The stride size, anchor size scale assigned to 6 detection layers in Figure 2.

Detection Layer	Stride	Anchor Size
D1	4	16
D2	8	32
D3	16	64
D4	32	128
D5	64	256
D6	128	512

### A.2. Training

During training, we adopt data pre-processing steps, augmentation strategies, and loss functions used in [21]. Specifically, we used color distortion by changing hue, saturation, value (brightness) of an image. Also, for generating various scales of faces, zoom-in and out operation are applied to image along with its face bounding boxes. Consequently, the resultant image is resized to  $640 \times 640$  after horizontal flipping. Also, max-out background label [21] is applied on D1 detection head for reducing false positives with regard to small faces. We also employed multi-task loss, where both classification and regression loss are normalized by number of positive anchors. We set balancing parameter between classification loss and regression loss as 1.

With regard to optimization hyper-parameters, we used ADAM [61] optimizer with initial learning rate 0.001, weight decay 5e-4, and batch size 32. The maximum number of iterations is 330k and learning rate is decayed at [250k, 300k, 320k] by 0.1.

### A.3. Evaluation

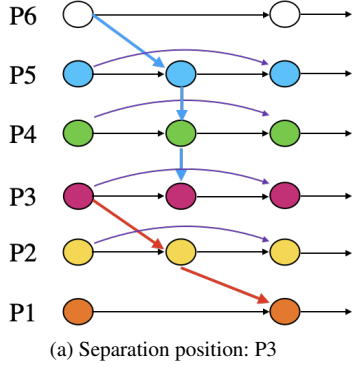
For evaluation on WIDER FACE, we employed flip and multi-scale testing [21], where all these predictions are merged by Box voting [56] with IOU threshold at 0.3. In case of using RetinaFace framework [9], we used single-scale testing where original image size is maintained.

## B. Stem Modification

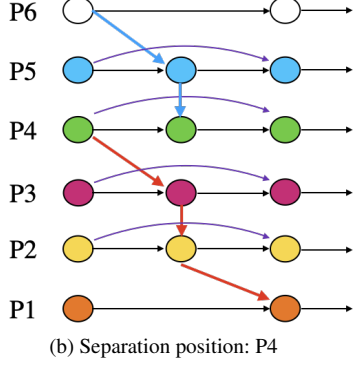
In Table 10, we compare detection performance depending on the design of stem layer. It is worth notable that our

Table 10. Latency and detection accuracy according to the stem design. We only changed stem layer of EResFD (Figure 2) with that of ResNet and our proposed stem design of EResNet.

Stem	ResNet	EResNet
Stem FLOPs	180.6 M	11.5 M
Stem Latency (Ratio)	24.1ms (42%)	4.5ms (12%)
Overall Latency	56.8ms	37.7ms
Easy mAP (%)	87.5	89.0
Medium mAP (%)	86.3	87.9
Hard mAP (%)	77.6	80.4



(a) Separation position: P3



(b) Separation position: P4

Figure 9. Architectures of SepFPN with various separation positions (P3, P4).

proposed stem layer requires much more reduced computational costs with significantly improved detection accuracy scores compared to that of ResNet.

### C. SepFPN

In Figure 9, we visualize the architecture of variations for our proposed SepFPN, where its separation position is varied from P3 to P4.